Elsevier Editorial System(tm) for International Journal of Fatigue
Manuscript Draft

Manuscript Number:

Title: Crack closure and fatigue crack growth near threshold of a metastable austenitic stainless steel

Article Type: Original Research Paper

Keywords: Fatigue crack propagation; Metastable austenitic Stainless steel; Crack closure; ΔK and Kmax; Martensitic Transformation

Corresponding Author: Dr. David Fernando Martelo Guarin, Ph.D

Corresponding Author's Institution: Research Institute for Materials Science and Technology INTEMA

First Author: David F Martelo Guarin, Ph.D

Order of Authors: David F Martelo Guarin, Ph.D; Antonio M Mateo, Ph.D; Mirco D Chapetti, Ph.D

Manuscript Region of Origin: The Americas

*Cover Letter

Mar del Plata, September 9, 2014

Prof. David McDowell, Co-Editor
International Journal of Fatigue

Dear Sr

Please find attached the manuscript of the paper "**Crack closure and fatigue crack growth near threshold of a metastable austenitic stainless steel**", which I submit to be reviewed for publication in the Journal "International Journal of Fatigue".

Hoping to hear from you soon, yours sincerely

David F. Martelo Guarin
Experimental Mechanics Laboratory
INTEMA
University of Mar del Plata - CONICET
J.B. Justo 4302
(B7608FDQ) Mar del Plata, Argentina

e-mail: martelo@fi.mdp.edu.ar

Highlights

- The Donald`s effect establish a good correlation between driving force and FCGR
- The strange values of ΔK_{th} found in MASS can be explained by the crack closure
- For this material the crack closure is induced by roughness
- To explain the load ratio effects in MASS is vital to include K_{max} and crack closure
- The influence of K_{max} and ΔK on the FCG vary with the change in the FCGR

Crack closure and fatigue crack growth near threshold of a metastable austenitic stainless steel

D. F. Martelo[a], A.M. Mateo[b], M.D. Chapetti[a]

[a] INTEMA, Research Institute for Material Science University of Mar del Plata-CONICET J.B. Justo 4302 (B7608FDQ) Mar del Plata Argentina

[b] CIEFMA, Departament de Ciència dels Materials i Enginyeria Metal•lúrgica Universitat Politècnica de Catalunya

Abstract

In this paper the fatigue crack propagation behavior of an austenitic metastable stainless steel AISI 301LN in the near threshold region is studied. The steel used in this research is investigated in two different microstructural conditions: annealed and cold rolled. The results obtained of the fatigue crack growth rate curves in the near threshold region are contrasted with previous results obtained in the same steel, but in the Paris region. This comparison shows that the mechanism that controls the fatigue crack advance in this material differ as a function of the level of ΔK applied, which is linked with the zone of austenite transformed to martensite. In the near threshold region, the load ratio effect cannot be completely explained by the concept of two driving forces, which seems to work in the Paris region. An alternative method is proposed to explain the contribution of the crack closure to the fatigue crack growth rate, based on the ASTM method and the ACR method proposed by K. Donald et al. According to the different analysis performed, the crack closure induced by roughness seems to be the main mechanism causing crack closure in this material. Finally, a new parameter to quantify the effective driving force and the influence of the load ratio is proposed, based on the two driving force concepts, the contribution of crack closure induced by roughness and the trajectory map proposed by K. Sadananda and A.K. Vasudevan.

Keywords : Fatigue crack propagation; Metastable austenitic Stainless steel; Crack closure; ΔK and K_{max}; Martensitic Transformation.

1. Introduction

The metastable austenitic stainless steels (MASS) are materials that have the martensitic transformation as distinctive feature, among others [1]. This transformation can be induced by stress or strain and it depends on many variables (i.e.

temperature, composition, stress, strain, strain rate, stress state, etc.) [2-3]. The particular microstructure of this kind of material is responsible for the high strain hardening and excellent ductility. These last two features make them highly desirable in the automotive industry.

Recently, the behavior of the MASS AISI 301LN (the material used in this investigation) under monotonic load has been studied in thin sheet of annealed and cold rolled specimens (the same conditions used in this investigation)[4-6]. The results showed an increase in yield stress with cold rolling, and better ductility in annealed condition [4-6]. However, it is not possible to extrapolate properties like yield stress to fatigue properties or to the fatigue crack propagation characteristics [7-8]. In thin walled components, the growth of a crack until a critical crack length constitute failure criteria [9] and since car components are subjected to cyclic loading, the use fracture mechanics parameters to characterize the fatigue life in thin specimen of MASS seems more appropriate.

The effects of martensitic transformation in the fatigue crack growth rate (FCGR) on MASS have been studied in the past [10-13]. However, to the best of the authors knowledge, there are only two studies of fatigue crack propagation behavior in the near threshold region [11, 14] and none in the near threshold region at temperature below the temperature of martensitic transformation of thin sheet specimens. The common conclusion of all these studies is that martensitic transformation decreases fatigue crack growth rates.

In a previous paper [15-16], it has been shown that the influence of crack closure in the FCGR of MASS is insignificant in the Paris region. In fact, in the literature there is not conclusive experimental evidence of crack closure induced by martensitic transformation. However, in the near threshold region other mechanisms that can induce crack closure become active, as crack closure induced by roughness [17].

This paper presents the results of fatigue crack growth tests in a MASS in the near threshold region. The results obtained from the assessment of the fatigue crack growth (FCG) behavior of the same steel used in this research but in the Paris region [15-16] will be also used. In particular, three observations will be considered. Firstly, the height of the zone of martensitic transformation around the crack increases with the increase of the range of stress intensity factor. Secondly, the maximum applied stress intensity factor (K_{max}) significantly contributes to the fatigue crack driving force. Thirdly, there is no experimental evidence that suggested the existence of a mechanism of crack closure induced by phase change.

This paper is similarly organized to paper [15-16] and the FCGR curves are plotted as a function of the same parameters that were used in the Paris region, which will be briefly introduced. Additionally, the FCGR curves obtained in the paper of reference [15-16] will be used. The main objective of this paper is to show that the effect of mechanical and microstructural variables that influence the FCGR in MASS can be explained taking into account both the traditional concepts of crack closure and the influence of the effects associated to the maximum value of the applied stress intensity value, K_{max}.

2. Specimen, material, and testing

Figure 1 shows the stress - strain behavior at room temperature of the MASS AISI 301LN used in this investigation. As it can be seen in **Figure 1**, in the annealed steel the material has a high strain hardening. This can be attributed to the composite strengthening generated by the martensite and to the increased dislocation density [18]. **Figure 1** also shows the stress - strain curve obtained at room temperature for the material in cold rolled condition (with the applied loading axis perpendicular to the rolled direction). The steel received in cold rolled condition has a yield stress higher than in annealed steel. Previous studies have shown that in cold rolled condition, the MASS AISI 301LN has a stress - strain curve that depends on the microstructure direction [4]. The stress - strain curve depends on, among other variables, the temperature and strain rate [19-20]. The chemical composition of the steels in annealed and cold rolled conditions is listed in **Table I**.

Table 1. Chemical composition (wt. %)

	Fe	Cr	Ni	Mo	C	Si	P	S	Mn	Cu	N
Annealed – 1 mm	Bal	17.86	6.42	0.24	0.015	0.471	0.031	0.007	1.495	0.173	0.094- 0.145
Annealed - 1.5 mm	Bal	17.98	6.78	0.23	0.012	0.548	0.031	0.004	1.562	0.057	0.094- 0.145
Cold-Rolled – 1.5 mm	Bal	17.94	6.30	0.18	0.016	0.513	0.032	0.005	1.481	0.135	0.094- 0.145

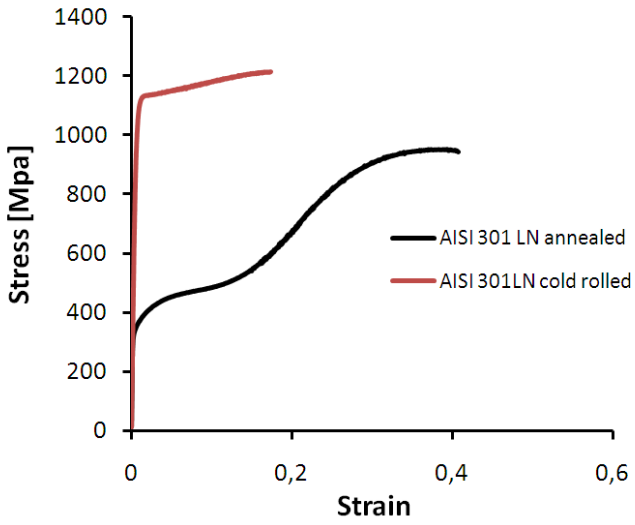

Figure 1. Stress-Strain curve for an AMSS in annealed condition and cold rolled condition.

The fatigue crack growth tests were carried out by using single edge notch tension (SENT) specimens. The SENT specimens of this study were obtained from thin sheets of 25 cm by 84 cm, which were machined using a water jet cutter. The specimens were designed as shown in **Figure 2**. Once the specimens were machined, one of their faces was electro-polished in a solution of 5%vol perchloric acid and 95% ethanol at 45 V.

On the other face of the specimen, the surface was abraded with silicone-carbide paper of 320-grit, to bond the Krak gages®. The Krak gage® is the sensor used to measure the crack length during the tests. The crack length was also

measured using the compliance technique by means of a clip gage in the crack mouth [21]. The fatigue crack growth tests were conducted in an Instron machine model 8801 with closed loop to computers for automatic test control and data acquisition. The specimens were held in wedge grips. The details of the solution for the stress intensity factor K of SENT specimens with wedge grips can be seen in reference [15- 16].

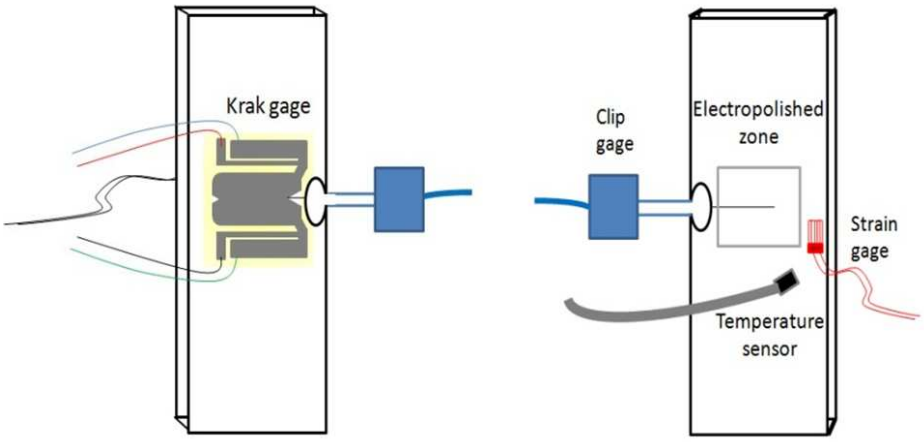

Figure 2. Schematic illustration of the SENT specimen used in this investigation with the Krak gage, the clip gage, the temperature sensor and the strain gage.

After fatigue tests, some of the specimens were used to observe the crack profile and the zone transformed to martensite around the crack, revealing the martensite by using a solution of 100 ml ethanol, 20 ml HCl, 1.5 g K_2S2O_5 and 2 g $NH_4F{\cdot}HF$. Two other techniques were used to detect the presence of martensite: micro-indentation and X-Ray diffraction. Other specimens were used to analyze the surface fracture in a scanning electron microscope.

The fatigue crack growth tests were conducted to a frequency of 20 Hz at room temperature, following the K-decreasing procedure [22]. In this type of tests the load decreases with the increase in the crack length. Two different types of test were implemented: tests with constant load ratio (R) and tests with constant $K_{max.}$ Because of no previous investigations on the fatigue crack growth behavior in the near threshold of thin sheet of MASS could be found, the effects of the load shedding rate (c parameter according to standard E647) were also evaluated.

The crack closure measurements were made using a procedure based on the ASTM offset method. In this modified method the slope (compliance and open-crack compliance) of the load – crack mouth displacement curve is taken from the average of the slope of the load and unload curve, in contrast with the ASTM method where the open-crack compliance is taken from the loading curve, and the compliance is taken from the unloading curve. The procedure is described in reference [15-16]. According to previous experience, an offset of 4% was used to determine the crack opening load (P_{op} or K_{op}).

3. Results

3.1. Fatigue crack growth rate curves in term of the range of stress intensity factor

Figure 3 shows the influence of the load ratio and the load shedding rate on the Fatigue crack growth rate *vs.* ΔK curve in the near threshold region of the annealed steel. The curves of **Figure 3** shows a decrease in the FCGR with the decrease of *ΔK*, as expected. The FCGR *vs.* ΔK curve is not influenced by the load shedding rate. One particular characteristic of the behavior showed by this material in the region near threshold is that the fatigue crack propagation threshold (ΔK_{th}) changes only a little from R = 0.1 until R = 0.5. When the fatigue crack growth tests were carried out at *R* superior than 0.7, the ΔK_{th} was almost half of the value obtained at lower *R*.

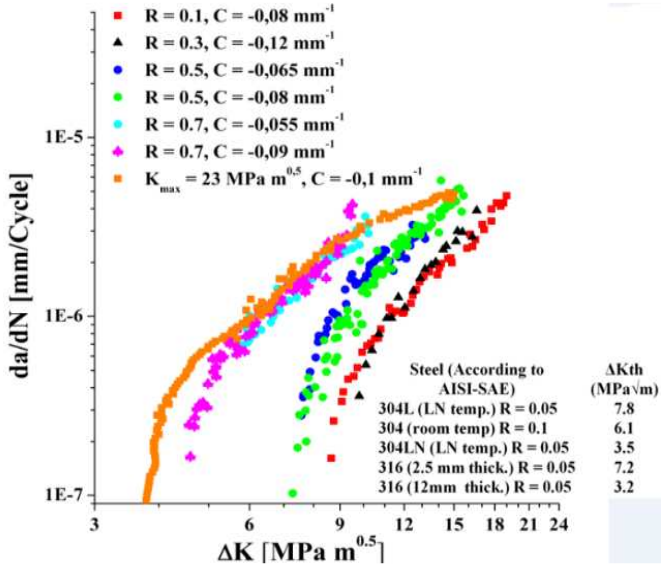

Figure 3. Fatigue crack growth rate *vs.* stress intensity factor range at different load ratio for the annealed steel.

Similar to the results obtained for the annealed steel, the FCGR is independent of the load shedding rate for the cold rolled steel, as it can be seen in Figure 4. For the cold rolled condition, there cannot be observed any influence of the crack plane orientation in the FCGR. For *R* superior to R = 0.5, the ΔK_{th} is almost independent of the load ratio. In fact, for *ΔK* lower than 10 MPa√m, the FCGR is almost independent of the *R* if *R* is higher than R = 0.5.

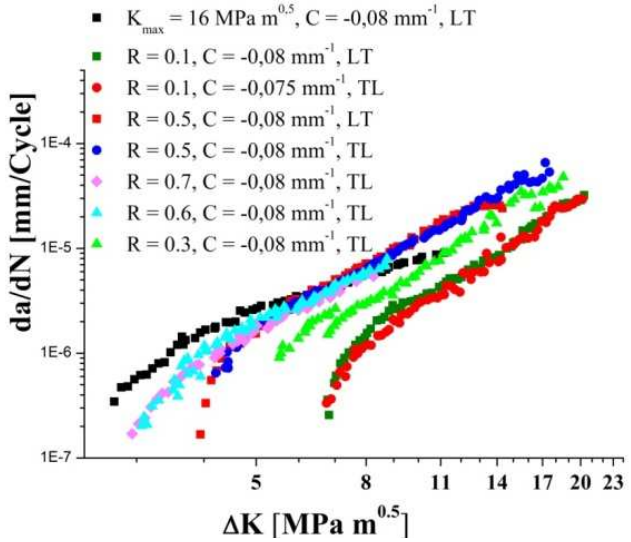

Figure 4. Fatigue crack growth rate *vs.* stress intensity factor range at different load ratio for the cold rolled steel.

3.2. Fatigue crack growth rate curves in terms of K_{eff} and the two driving force parameters

The traditional explanation of the load ratio effects is based on the crack closure concepts, firstly proposed by W. Elber [23]. The crack closure implicates that there is a premature contact between the cracks faces though that the applied load is tensile; therefore, the effective fatigue crack driving force is reduced. In this paper three methods to calculate the ΔK_{eff} will be used. **Figure 5** shows the variation of the level of crack closure as function of ΔK, where P_o is the load point where the crack faces make contact and P_{max} is the maximum applied load. The level of crack closure increase as ΔK approaches to ΔK_{th} becoming of the order of 85% in the relationship P_o/P_{max}. However, a unique relationship between ΔK and P_o/P_{max} for R constant test cannot be established. This is problematic if the load ratio effects want to be correlated in terms of the effective stress intensity factor (ΔK_{eff}), as it will be shown in **Figure 6**b.

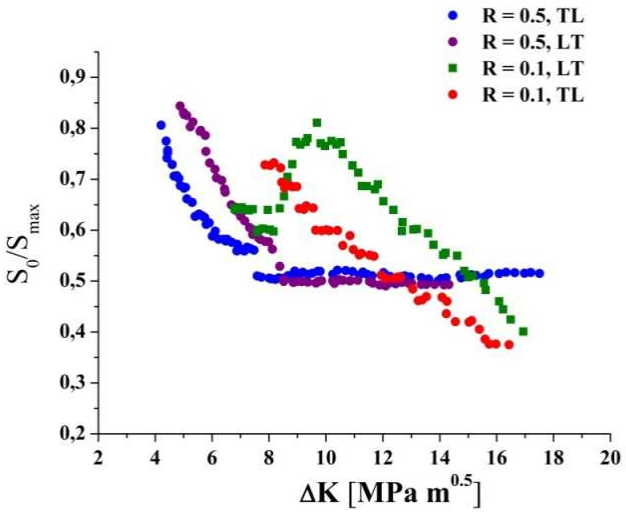

Figure 5. Variation of the relation P_o/P_{max} for test conducted at constant R for the steel in cold rolled condition.

Figure 6a shows the variation of the FCGR *vs.* ΔK_{eff} for the annealed steel. Defining ΔK_{eff} as in equation (1) and determining K_{op} as in paper [15-16], in this figure the curves tend to approach.

$$\Delta K_{eff} = K_{max} - K_{op} \quad (1)$$

However, it is still not possible to gather together all the curves into a master curve. A similar situation is found in **Figure 6**b which shows the plot of FCGR *vs.* ΔK_{eff} for the cold rolled steel. **Figure 6**b shows that even if a relationship between ΔK and FCGR for R constant test can be established, it cannot be done in terms of ΔK_{eff}, as it is shown in the curves of the tests conducted at R = 0.5. Another problem is found in the curve of the test for R = 0.1 in the cold rolled steel when ΔK_{eff} is used as driving force, **Figure 6**b. In this curve the FCGR decreases with the decrease in ΔK_{eff} until ΔK_{eff} = 2.6 MPa, from which an apparent increase of ΔK_{eff} results in a continuous decrease in FCGR. The fatigue crack growth tests at K_{max} constant for the annealed and cold rolled specimens do not show crack closure.

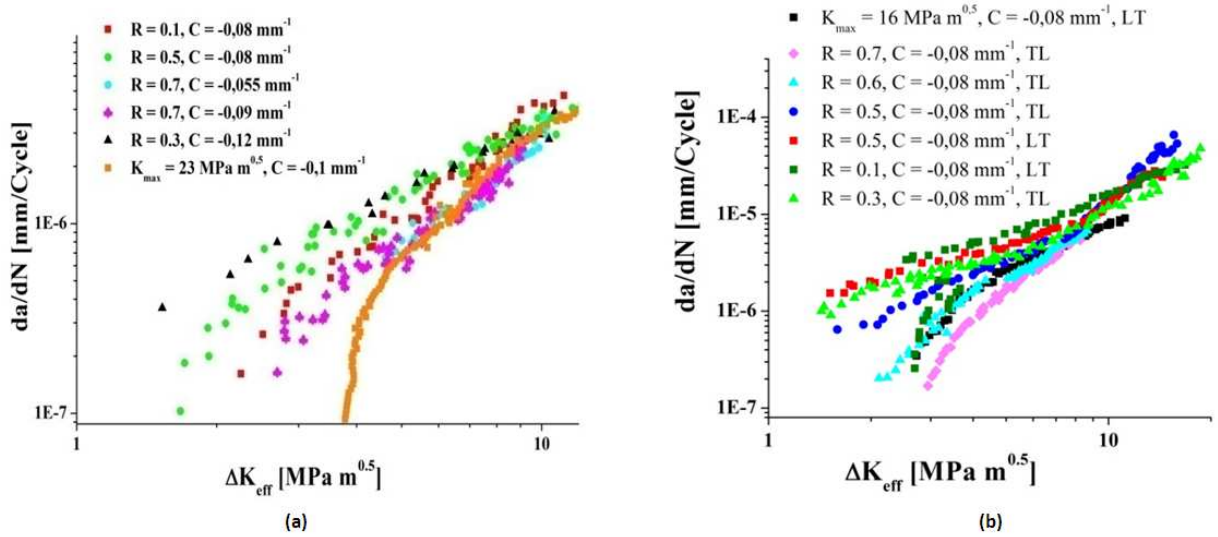

Figure 6. Fatigue crack growth rate as a function of the effective stress intensity factor for (a) the annealed steel, and (b) cold rolled steel.

Considering that the interference of crack surfaces do not completely shield the crack tip from fatigue damage, K. Donald *et al*. [24] have proposed to calculate an effective stress intensity factor range as:

$$\Delta K_{2/PI} = \Delta K_{app} - \frac{2}{\pi}(K_{op} - K_{min}) \quad (2)$$

Figure 7 shows the relationship between FCGR *vs.* ΔK_{eff} according to the proposal of K. Donald *et al.* for the annealed steel, **Figure 7**a, and for the cold rolled steel, **Figure 7**b. Even though the Donald`s effect does not make the FCGR curves

collapse, this parameter is able to establish a good correlation between driving force and the FCGR for tests conducted at different *R* for the specimens in annealed and cold rolled states. The problem of the rationalization of the load ratio effects using the donald`s effect is that the same inconvenient previously found using the traditional concepts of crack closure still persists.

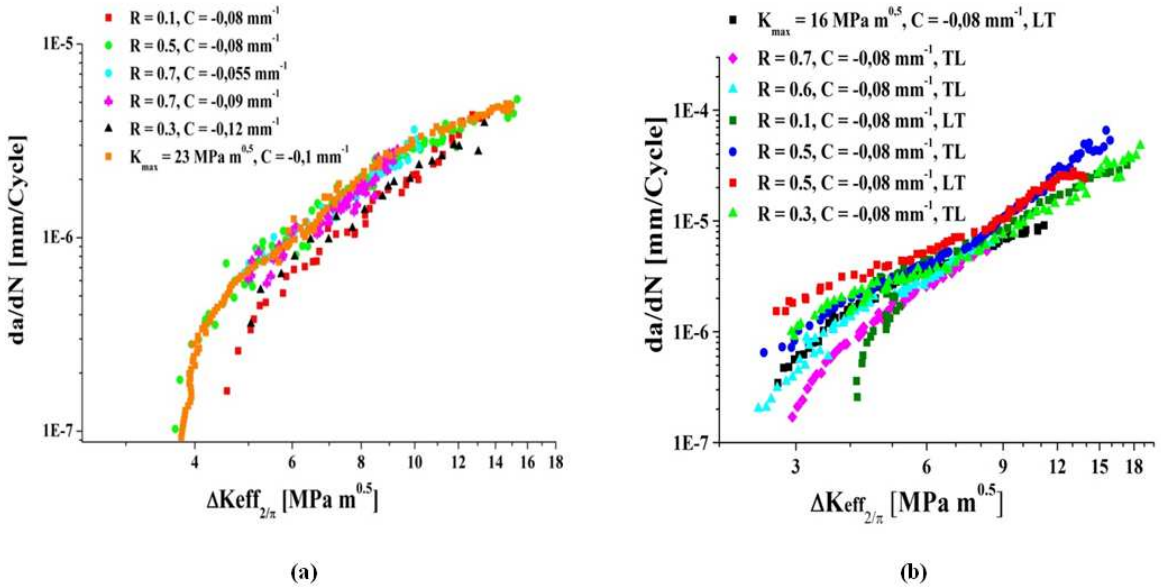

Figure 7. Fatigue crack growth rate as a function of the effective stress intensity factor proposed by K. Donald et al. (a) for the annealed steel and (b) the cold rolled steel.

Since the explanation of the load ratio effects based on crack closure presents some inconsistencies like those previously shown and other shown in other papers [25-27], and taking into account the necessity to relate the FCG behavior as a function of a proper driving force, D. Kujawski proposed a crack driving force parameter, K*, that is calculated by using K_{max} and the positive part of the range of stress intensity factor (ΔK^+), as follows:

$$K^* = (K_{max})^{\alpha}(\Delta K^+)^{1-\alpha} \quad (3)$$

Note that in order to describe uniquely a fatigue cycle two independent loading parameters are neccesary. In Kujawski`s parameter the contribution of K_{max} and ΔK^+ is determined by the α value, which depends on the material properties and the test conditions, among others variables. **Figure 8** shows the relationship between FCGR *vs.* K* in the near threshold region for the annealed steel and the cold rolled steel. To correlate the load ratio effects in this region, the α value that was found in the Paris region for each material [15-16] was used, **Figure 8**c and d. The results show that in the near threshold region the Kujawski`s parameter is not as successful as in the Paris region, as it can be observed in **Figure 8**a and b. However, the correlation can be improved using an α value equal to 0.5, as it can be observed in **Figure 8**e and f. In any case, the results obtained are not as successful as in the Paris region.

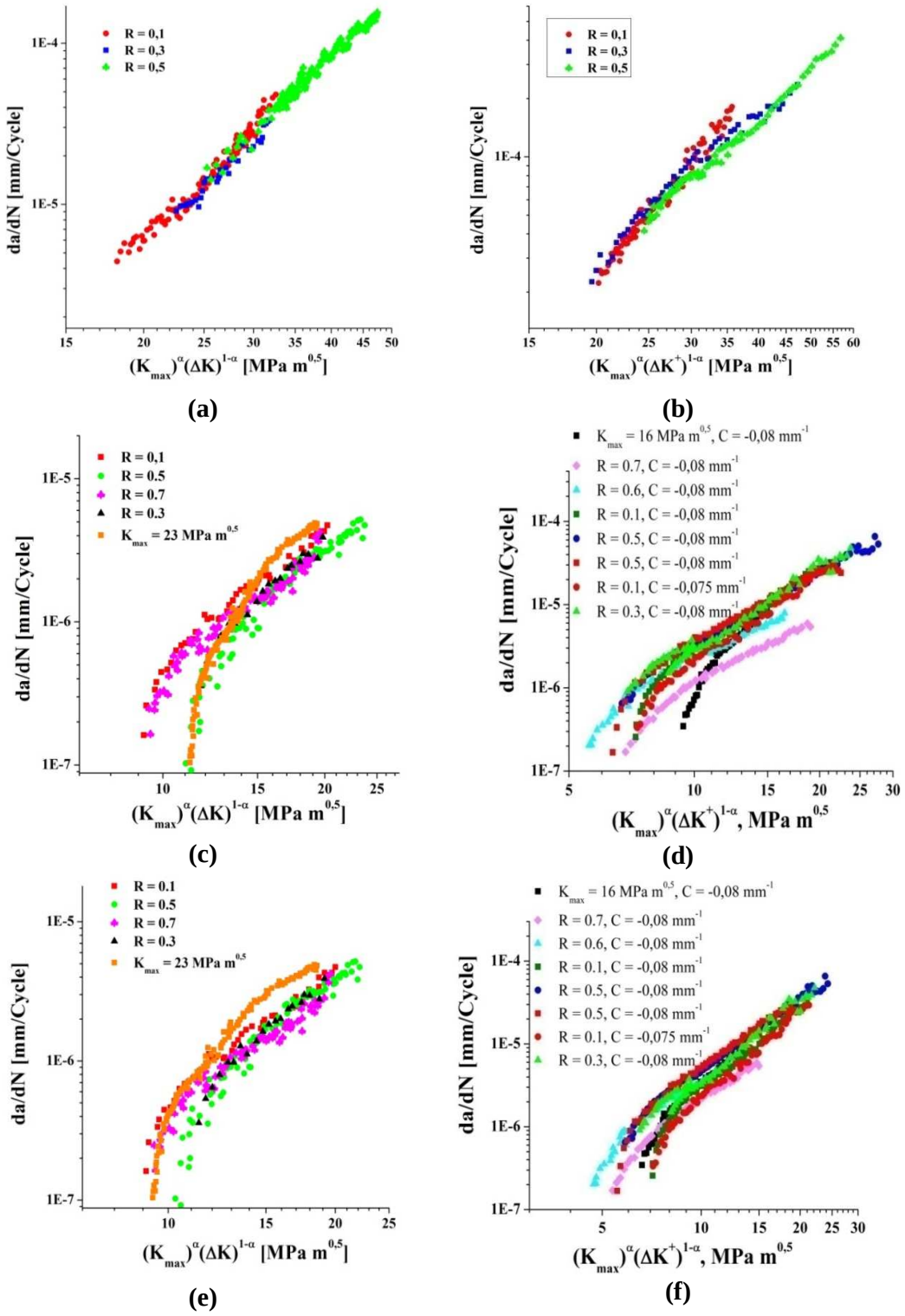

Figure 8. Fatigue crack growth rate as a function of the Kujawski`s parameter for (a) the annealed steel in the Paris region with α equal to 0.6, and in the near threshold region with (c) α equal to 0.6 and (e) α equal to 0.5. Also, for the cold rolled steel (b) in the Paris region with α equal to 0.7, and in the near threshold region with (c) α equal to 0.7 and (e) α equal to 0.5.

3.3. Martensitic transformation zone

Figure 9 shows the diffractograms obtained from the surfaces fracture of specimens tested in the near threshold region. The results of the x-ray analysis showed peaks of austenite and martesite, which indicate that in the region corresponding to the crack path the martensitic transformation is incomplete for both conditions (annealed and cold rolled). The same result obtained by x-ray diffraction analysis was confirmed by etched. **Figure 10** shows that even at high K_{max} in the near threshold region (low ΔK); the martensitic transformation is limited to the area of the characteristic microstructural size.

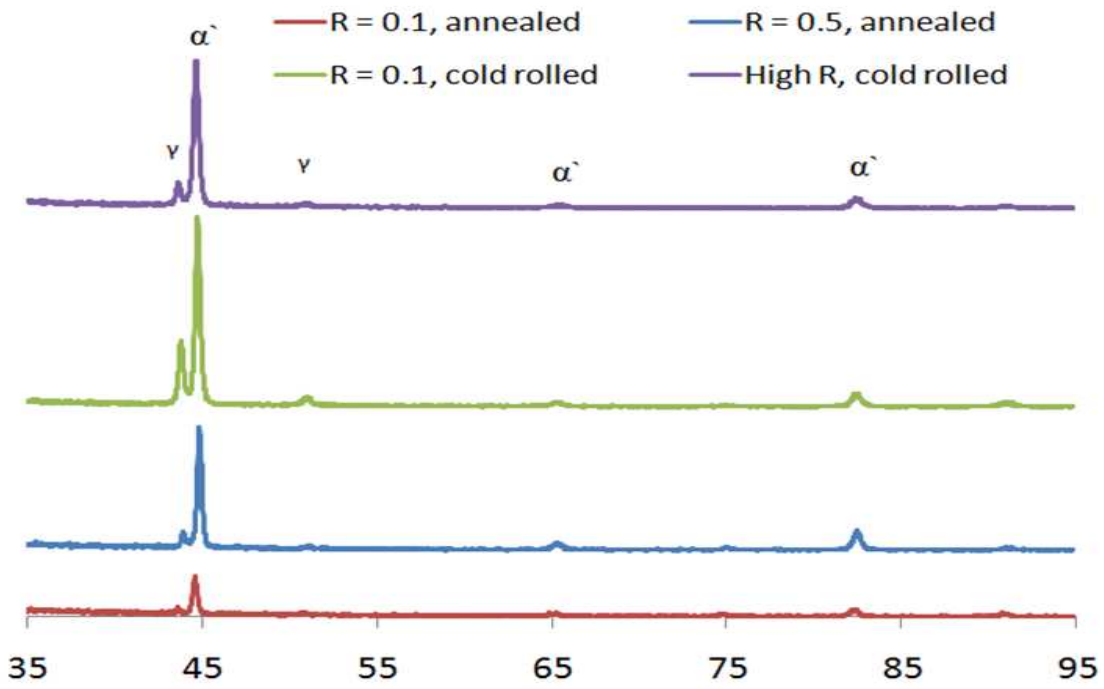

Figure 9. X-ray diffraction spectra of the fracture surface in annealed and cold rolled condition.

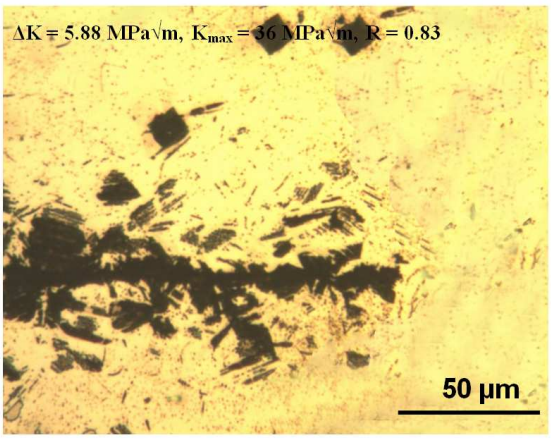

Figure 10. Optical micrograph of the fatigue crack profile of the annealed steel showing the martensite phase in black.

4. Discussion

Studies of different authors [28-30], and particularly the studies of A.K. Vasudevan and K. Sadananda [31-32], have proved the necessity of including the K_{max} as a true driving force for the fatigue crack growth (FCG). By using the two driving force parameters of Kujawski, it was possible to correlate adequately the load ratio effects in a MASS in annealed condition and cold rolled condition in the Paris region, Figure 8 (a) and (b). However, in the near threshold region the driving force of Kujawski is not as successful as in the Paris region. In fact, the results obtained in this region for the MASS do not show the typical K_{max} dependence observed in most common metallic alloys. For example, the ΔK_{th} at R = 0.1 is lower than the ΔK_{th} at R = 0.3. This peculiarity becomes more evident if the FCG behavior in the threshold is represented using a ΔK_{th} *vs.* K_{maxth} curve, proposed by A.K. Vasudevan *et al.* [33]. **Figure 11** shows the fundamental threshold curve obtained for the MASS in annealed condition. If the classification proposed by A.K. Vasudevan *et al.* is used, this material in annealed condition has a tendency to behave as a class V behavior, which differs from the other classes by the increase in the fatigue resistance with the increase in the K_{max}. This type of behavior has not been found in metallic alloys, only in some polymer materials like polycarbonate, rubber modified polystyrene and polyvinylchloride. In these materials, this behavior could be attributed to the rearrangement of the polymer chains to become stronger. However, in metals, that behavior could only be caused by extrinsic factors, like the crack closure. For the present materials the crack closure is detected both in the region near threshold and in the Paris region.

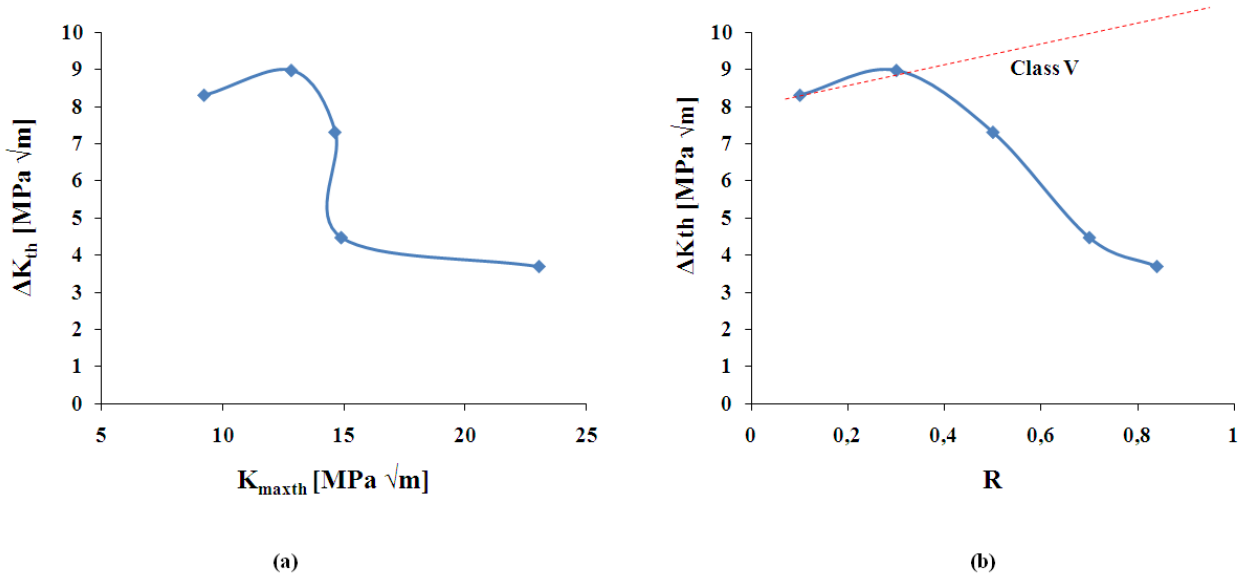

Figure 11. (a) Fundamental threshold curve for the annealed steel (b) Variation of the ΔK_{th} *vs. R*, showing an atypical class V behavior.

4.1. Influence of crack closure

Table 2 shows the measurements of the crack opening load for tests conducted on the Paris region in both conditions. The

results indicate that for this steel the crack closure is independent of the austenite stability. Therefore, for this steel in the Paris region the crack closure is caused by plasticity or by roughness or by a combination of both mechanisms. However, the point to point variability of the crack closure measurements and because the estimation of the crack opening displacement is on the same order of magnitude than roughness (see **Figure 12**), it may be assumed that for this steel the crack closure is caused only by roughness in the Paris region.

Table 2. Crack opening stress for a thin sheet of 1.5mm thickness of an AMSS at R = 0.1 but for different test temperatures.

	R = 0.1 Cold rolled T = 80°C	R = 0.1 Cold Rolled T = 24°C	R = 0.1 Annealed T = 80°C	R = 0.1 Annealed T = 24°C
P_o/P_{max}	0.24-0.28	0.28-0.33	0.24-0.28	0.24-0.28

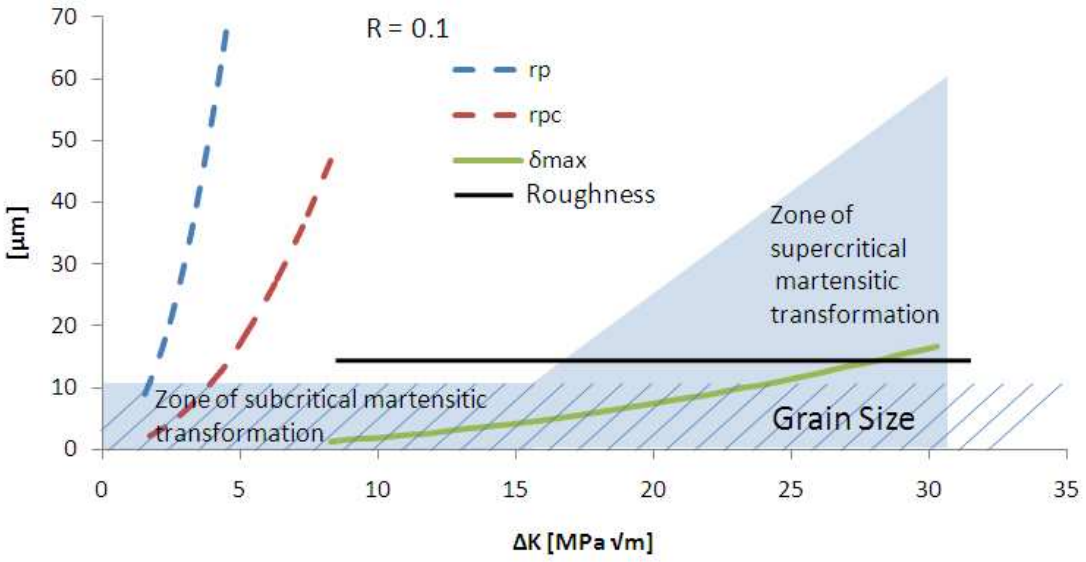

Figure 12. Representation of the size of the microstructural characteristic dimension and from the monotonic (r_p) and cyclic (r_{pc}) plastic zones and the maximum crack tip opening displacement.

According to **Figure 6**, **7** and **8**, the driving forces based on crack closure are more successful to explain the load ratio effects than the Kujawski`s parameter in the region near threshold, whereas the ΔK_{eff} proposed by K. Donald *et al*. is more successful in explaining the load ratio effects than the ΔK_{eff} proposed by W. Elber. Since the plastic zone in front of the crack tip is limited when ΔK is near ΔK_{th}, the contribution to the crack closure by plasticity is limited in the region near the threshold. Besides, the results from the compliance measurements in the Paris region, where the martensitic transformation was extensive next to the crack, indicate that there is no crack closure induced by phase transformation. Therefore, it may be assumed that for this steel the crack closure is caused only by mechanisms of crack closure specific to this region such as oxide or roughness. Of these two mechanisms, roughness induced crack closure appears to be the most dominant as, for

example, for the same R at the same ΔK or the same range of crack mouth opening displacement, the relationship between P_o/P_{max} is always higher for the specimens in annealed condition, which have a higher roughness. However, unlike what happens in the Paris region, in the near threshold region the crack closure seems to play a significant role in the FCGR of MASS.

As mentioned before, the FCG behavior of this annealed steel in the near threshold region is not what is usually observed for metallic alloys. Without invoking the controversy of the FCGR dependency in K_{max} and without expecting ΔK_{eff} to be the only driving force for FCG; if the crack closure mechanism shields the crack tip from the fatigue damage changing its intrinsic behavior, the crack closure measurements should be higher for the load ratios R = 0.3 and R= 0.5 than the measurement obtained at R = 0.1. **Table 3** shows measurements of the ΔK_{eff} obtained at threshold and the relationship P_o/P_{max}. Both relationships show that the reduction in the crack driving force (ΔK_{eff}) by the crack closure is higher at R = 0.3 and R = 0.5 than at R = 0.1. To prove if the crack closure in the MASS in annealed condition was related to roughness mechanism, the fatigue crack profiles were analyzed. **Figure 13** shows two SEM micrographs of the crack profile near threshold at R = 0.1 and R = 0.5. The complete analysis of the crack profiles at different load ratios show no significant differences in the roughness for all load ratios studied. Based on the roughness analysis, an increase in K_{op} in the tests carried out at R = 0.3 and R = 0.5 would not be expected to occur. A. J. McEvily et al. [34] have also described the response of materials in the region near threshold but based on the crack closure. The analysis of A. J. McEvily et al is used to try to establish the source of crack closure for the material of this research. However, according to these authors, if the crack closure were caused by roughness, the value of K_{op} should be equal for all load ratios. As is shown in **Table 3** this situation does not occur. Therefore, and since no similar results could be found in the literature, it is concluded that for this material, the crack closure could be induced by roughness in combination with a closure mechanism specific of this material.

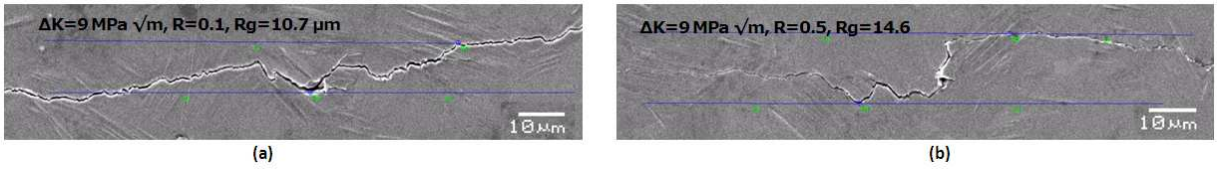

Figure 13. SEM micrograph of the crack profile in the annealed steel (a) at R = 0.1 (b) R = 0.5.

Table 3. Relationship between ΔK_{eff}, K_o/K_{max} and K_{op} *vs.* R.

	R = 0.1	R = 0.3	R = 0.5	R = 0.7
ΔK_{eff}	2.2	1.5	1.6	2.6
K_o/K_{max}	0.76	0.88	0.88	0.82
Kop*	7.3	12	13.4	12.8

* For a FCGR of 3.6×10^{-7} (mm/cycle)

It can be seen from **Figure 6**, and taking as reference the curves without closure (test conducted at K_{max} = 23 Mpa √m in

the annealed steel and K_{max} = 16 Mpa √m for the cold rolled steel), it may be said that the ΔK_{eff} proposed by W. Elber overestimates the contribution of crack closure in the decrease of the FCGR. These results agree with the analysis of A.K. Vasudevan *et al.* [35], which considers that when crack closure is induced by roughness, its contribution to the decrease in ΔK_{eff} is lower than expected, according to the ΔK_{eff} proposed by W. Elber. His hypothesis states that below the point where the crack faces make contact, there is not fatigue damage. Somehow, the analysis of Vasudevan *et al.* is analogous to the Donald`s effect. Both analyses consider that the fatigue damage occurs even when the crack faces are in partial contact. In line with this rationalization, the analytical estimation of the contribution of crack closure depends on the crack faces point-to-point interactions. For this reason, a unique function to describe the contribution of closure to FCG for all cases would be impossible. For this material in cold rolled condition, the main inconvenient of using ΔK_{eff} as driving force is that it could not establish a unique relationship between ΔK_{eff} and FCGR for a given load ratio, as clearly shown in **Figure 14**. To analyze this situation, the ACRn2 method proposed by K. Donald *et al.* [29] to determine the ΔK_{eff} is used.

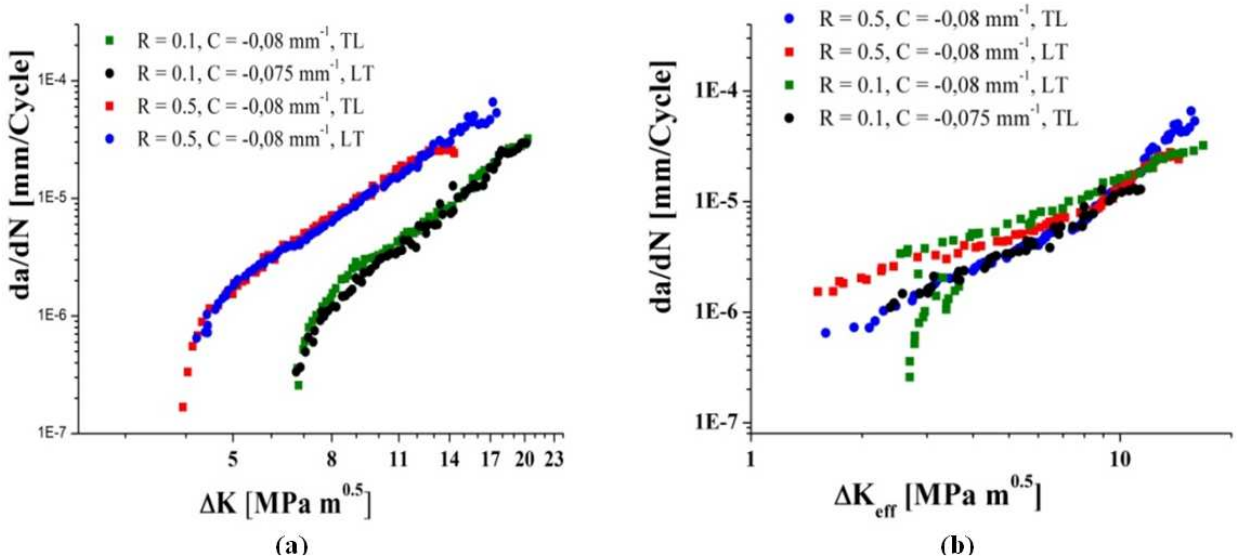

Figure 14. Fatigue crack growth rate of the cold rolled steel at R = 0.1 and R = 0.5 (a) as a function of ΔK (b) as a function of ΔK_{eff}.

The ACRn2 method [24] calculates the ΔK_{eff} through the relationship between real crack mouth opening displacement (whenever it uses a clip gage in the crack mouth of the specimen), and the crack mouth opening displacement that would occur without crack closure. This method differs from the ACR method in the assumption that the force distribution should be greater near the crack tip, while the ACR method assumes that the force distribution on the crack wake surfaces is fairly uniform. A more detailed explanation o this method is found in [24]. The ACR and the ACRn2 method were proposed to have into account the contribution of the load below K_{op}, to FCG, an idea similar to the Donald`s effect. Unlike to the Donald`s effect, this method is not based in the determination of a minimum change in the compliance curve, but in the relation between the real range of the crack mouth opening displacement and the range of the crack mouth opening

displacement without closure [29]. The numerical results of both methods were compared in paper [24] for two aluminum alloys, and the comparison show that the results obtained by both methods were similar. However, as the calculation of the ACRn2 is not based on the determination of K_{op}, the analysis of the load versus displacement curve could give some information about the anomalous results exposed in **Figure 14**.

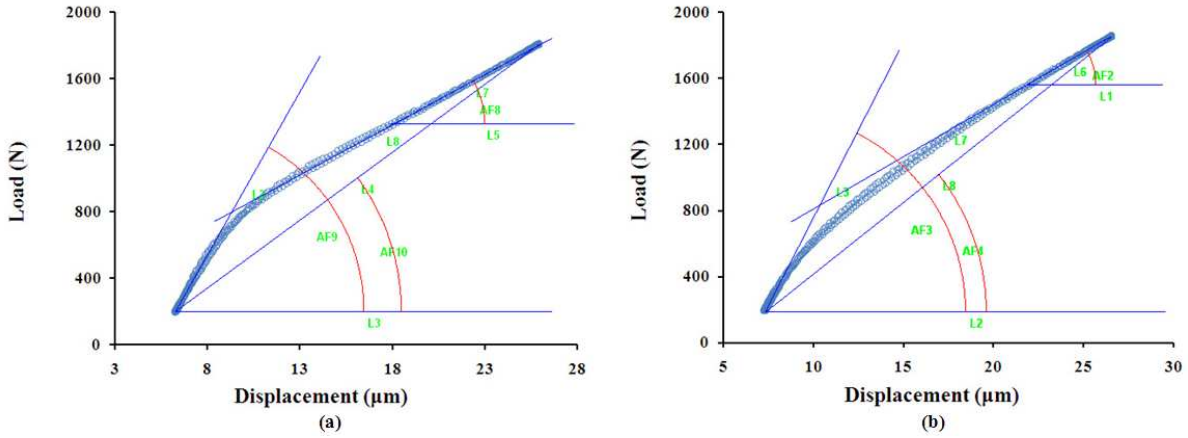

Figure 15 shows two load *vs.* displacement curve obtained for the MASS in cold rolled condition at a ΔK = 10.3 MPa√m at R = 0.1 but for different crack plane orientations. **Figure 15**a shows a change in the slope of load *vs.* displacement curve more noticeable than the one observed in **Figure 15**b. The results obtained from the ACRn2 method are shown in table II and compared with the $K_{op.}$ Because of the ACRn2 does not provide values of K_{op}, a mathematical artifice was used to convert ACRn2 in K_{op}, shown schematically in Equation 5.

$$\Delta K_{eff} = ACR_{n2}\Delta K \quad \textbf{(4)}$$

$$K_{op} = K_{max} - \Delta K_{eff}$$

$$\text{Then, } \frac{K_{op}}{K_{max}} = \frac{K_{max}-\Delta K_{eff}}{K_{max}} = \frac{K_{max}-ACR_{n2}\Delta K}{K_{max}} \quad \textbf{(5)}$$

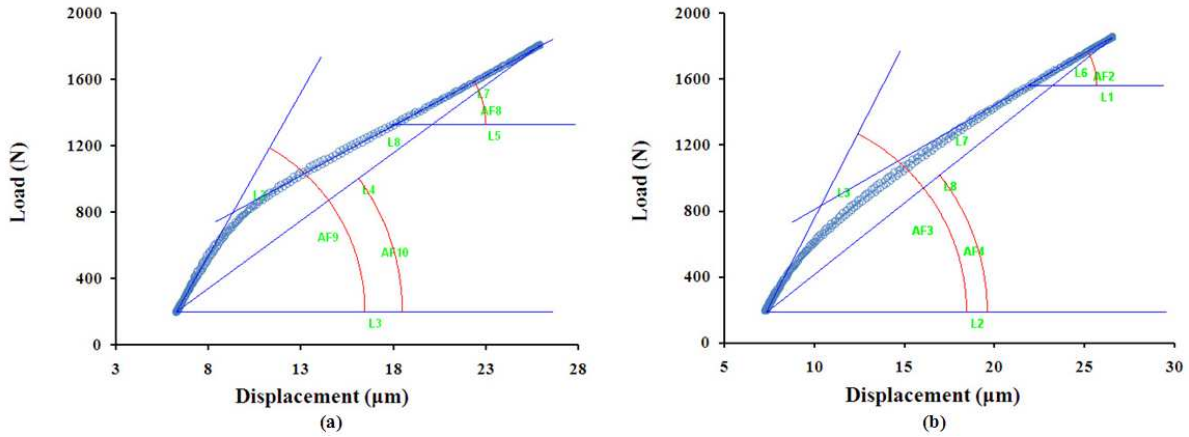

Figure 15. Load against crack opening displacement for the cold rolled steel in near threshold at R = 0.1 (a) TL orientation (b) LT orientation.

Table 4. Crack opening stress calculated using the m ASTM method and the ACRn2 method.

	Po/Pmax (mASTM method)	Po/Pmax (ACRn2 method)	Rougness (µm)
ΔK = 10.3 MPa √m, R = 0.1, TL	0.55	0.44	4.3
ΔK = 10.3 MPa √m, R = 0.1, LT	0.77	0.43	7.2

Table 4 shows the results obtained from the ACRn2 method and the modified ASTM method. No noticeable difference in the relationship P_o/P_{max} for the test with different crack plane orientations was observed when compared in terms of the ACRn2 method. This result would explain why curves correlate well in terms of ΔK and not of ΔK_{eff} (defined according to the method used in this work). To understand why the ASTM method with the modification proposed in this work give different values of K_{op} for the steel with different crack plane orientations, the crack profile must be analyzed. **Figure 16** shows optical micrographs of the fatigue crack profile propagated in the near threshold region of an MASS in cold rolled condition. From all conditions tested (annealed in the Paris and in the near threshold regions and cold rolled in the Paris and in the near threshold regions), the roughness in the near threshold of the cold rolled steel was the lowest. However, in the specimens with crack plane orientation LT found peaks of roughness almost twice higher than the ones observed in specimens with crack plane orientation TL. This could be the reason why the K_{op} detected with the modified ASTM method was higher for the steel in crack plane orientation LT.

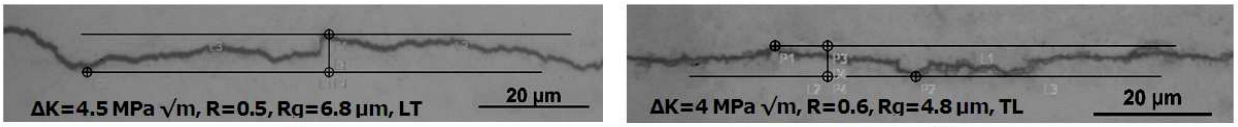

Figure 16. Optical micrograph of the crack profile in the cold rolled steel (a) at R = 0.5 LT orientation (b) and R = 0.6 TL orientation.

4.2 Crack path profile analysis

As shown in **Figure 13** and **Figure 16**, in the region near threshold the crack path roughness is higher for the MASS in annealed condition compared to steel in cold rolled condition, likewise, the peaks of roughness found are bigger in the annealed specimen compared to the cold rolled specimens. The decrease in the fatigue crack roughness with the cold rolled process in the near threshold region has been cited previously [36]. However, the explanation to this phenomenon is not clear. In dual phase steels with continuous martensite phase, the pre-strain cause a reduction in the resistance to the crack growth of the martensite phase. In this context, the crack passes directly through the martensite phase [37]. This could be the case of cold rolled specimens in this research. Whatever the explanation, this could be a factor used to explain the difference in the FCGR of the annealed and cold rolled specimens in the near threshold region. However, to consider the effect of crack roughness quantitatively is a very difficult task. This is because the analytical methods used to estimate the effects of crack deflection consider that the kink length must be bigger than the cyclic plastic zone; a condition rarely observed in plane stress conditions, as found in thin sheet specimens.

4.3. Surface fracture

Another factor that can be used to explain the differences in the FCGR between the steel in annealed and cold rolled condition is the influence of the fracture mode. For the annealed steel in the near threshold region, the fracture surface is composed by flat facets immersed in a region very irregular in appearance, as it can be seen in **Figure 17**a and b. The fracture surfaces in the near threshold region are very similar regardless of the level of K_{max}. In fact, the fracture surfaces obtained in this region are very similar to the one obtained in the Paris region at R equal to 0.1 [15-16]. The only difference is that in the threshold region the flat facets are more numerous. In previous studies, the flat facets have been attributed to separation along the twin boundary [38]. This new preferential path for the crack growth has been attributed to the decrease in the zone transformed to martensite around the crack path rather than to decrease in ΔK, although, the decrease in region transformed to martensite is caused by the decrease in ΔK.

The morphology of the surface fracture obtained in the near threshold region in the cold rolled steel differs from the obtained in the annealed steel. In this region the surface fracture is homogeneous at lower magnification (see **Figure 17**c), but similar to the irregular region of annealed steel at higher magnification (see **Figure 17**d). The main characteristic of crack path in this region is that is very straight.

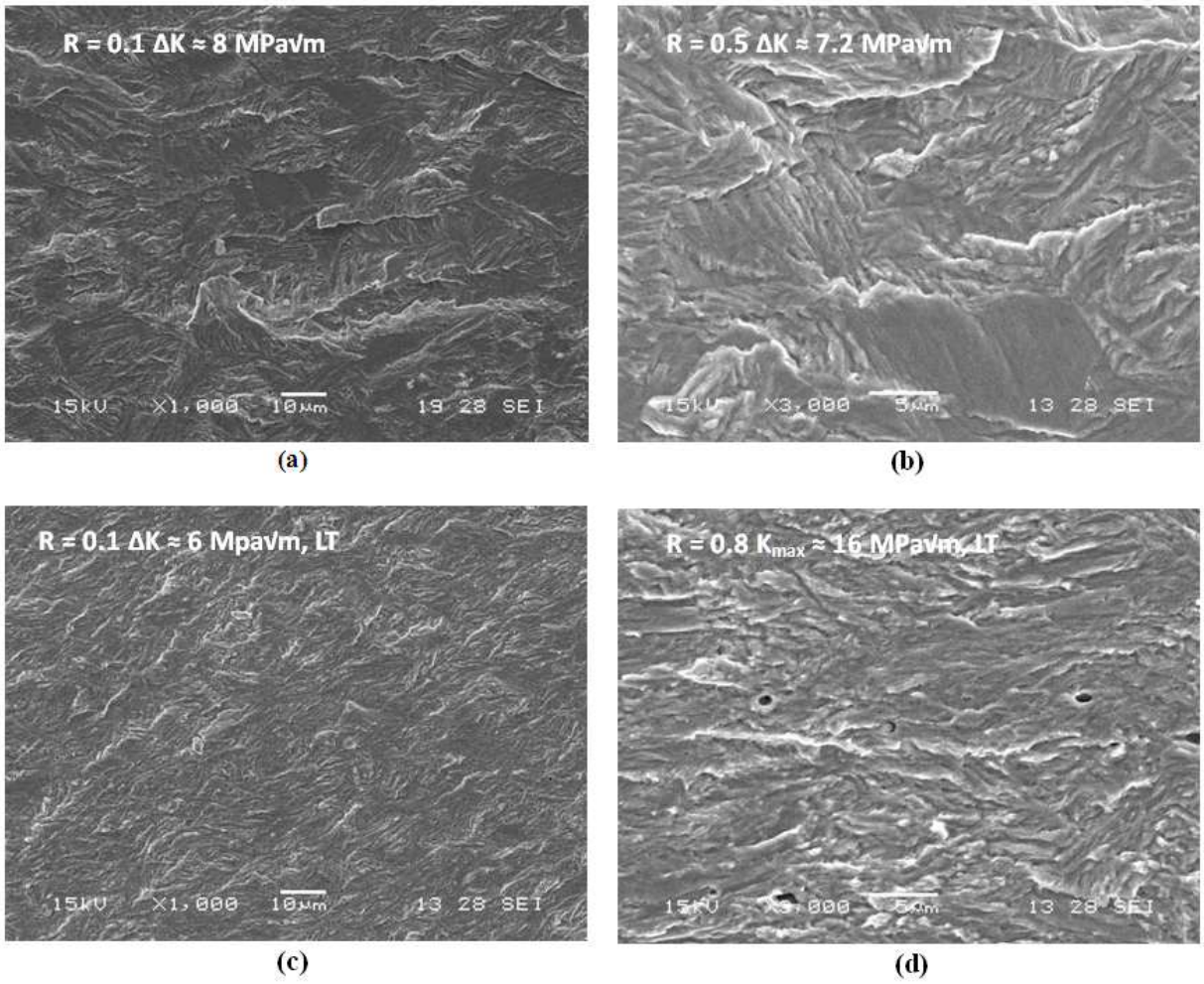

Figure 17. SEM image of the fatigue fracture surface corresponding to (a) and (b) annealed condition, (c) and (d) cold rolled condition.

The analysis of the mechanism that could interact in the FCG behavior in a MASS reveals, that in the near threshold, the mechanism of crack closure induced by the periodic deflection in the crack path is the main source of retardation (in addition to K_{max} which is a driving force inherent to the fatigue crack growth process). This analysis also reveals that, in order to quantify the crack closure induced by roughness, other methodologies that the one proposed by the ASTM (which is based on the concept of Elber) are necessaries

5. New Proposal. Correlation of the load ratio effects

Figure 18 summarizes the effect of the mechanical and microstructural variables on the FCGR of MASS. This Figure shows that the FCGR can be related in terms of the range of stress intensity factor (as in most metallic alloys), and that the two main variables that influence the FCGR are the load ratio and the martensitic transformation (as previous studies in MASS have shown). Also, different approaches used to explain the effect of mechanical and microstuctural variables in the FCGR (including the peculiarities that the material under study in this investigation has presented) are shown. Based

on this analysis, a parameter capable of correlating all the FCGR curves into a master curve is proposed.

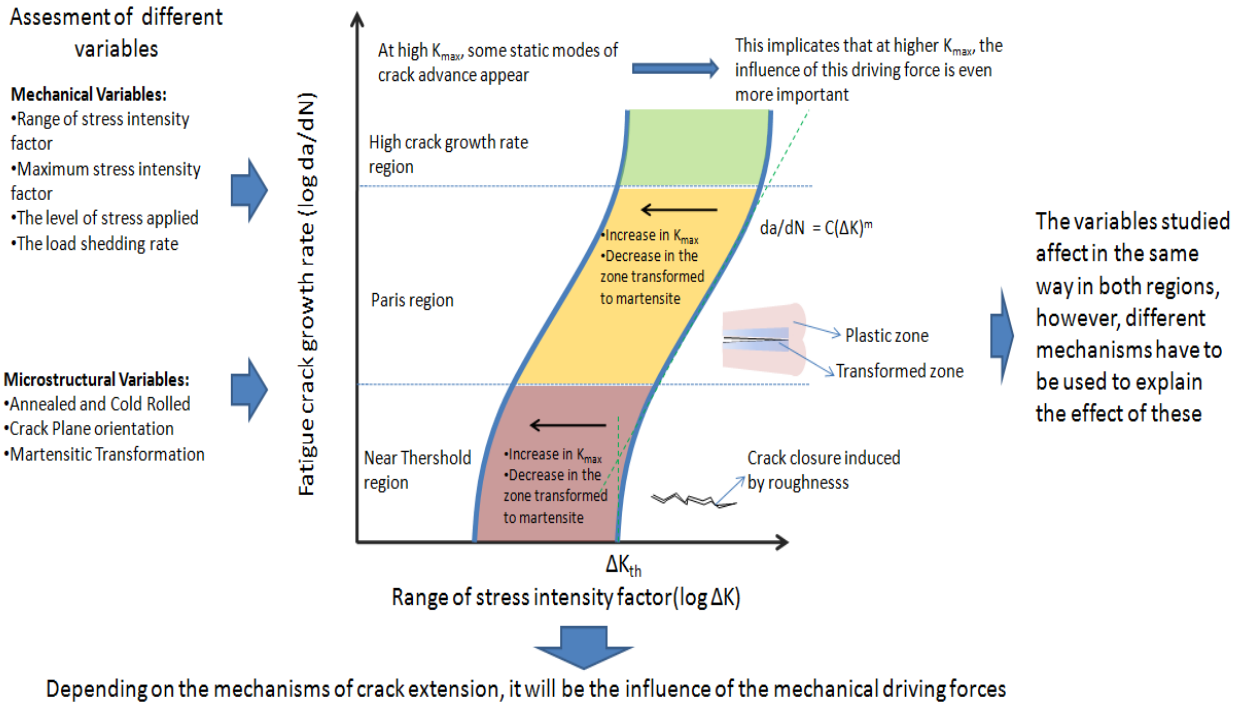

Figure 18. Schematic summary of the variables studied in this work, and the effect of these on the FCGR of an MASS.

Analyzing the results obtained in terms of the Kujawski`s parameter, the important role of parameters ΔK and K_{max} in the fatigue crack growth changes with the variation in the FCGR can be appreciated. The variation of the contribution of these parameters to the crack advance reflects the alteration in the mechanism that controls FCG. In the steel studied in this investigation the mechanisms of crack growth are largely affected by the microstructural changes (martensitic transformation). The fact that the influence of K_{max} and ΔK on the FCG vary with the change in the FCGR have been studied by K. Sadananda *et al.* [39]. These authors have proposed the analysis of this change in the mechanism of crack growth in terms of the driving forces, by using the trajectory map. One approach for correlating the load ratio effects including the change in the mechanism of crack growth is proposed in this paper, as follows:

$$\boldsymbol{K^{**} = (K_{max})^{\alpha_m}(\Delta K^{+})^{1-\alpha_m}} \quad \textbf{(6)}$$

where α_m has the same physical meaning than the α parameter in Kujawski`s equation. For the MASS in annealed state, the parameter α_m varies between 0.6 in the Paris region (Complete martensitic transformation of the microstructure adjacent to the crack path) and 0.4 in the near threshold region (Partial martensitic transformation of the microstructure adjacent to the crack path). The value of α_m equal to 0.4 in the near threshold is obtained from the results from studies by S. Kalnaus *et al.* [40] who determined the value of α for an austenitic stainless steel at temperature of no martensitic transformation in the Paris region. Mathematically, the parameter α_m can be represented by the hyperbolic function shown

in **Figure 19**. The correlation of load ratio effects obtained using the equation (6) is shown in **Figure 19**. Though that equation (6) is obtained only from macroscopic parameters and without using the crack closure data, the results obtained using this equation give a good correlation of R effects. However, and since the effects of the crack closure cannot be denied for this material, the equation (6) is incomplete.

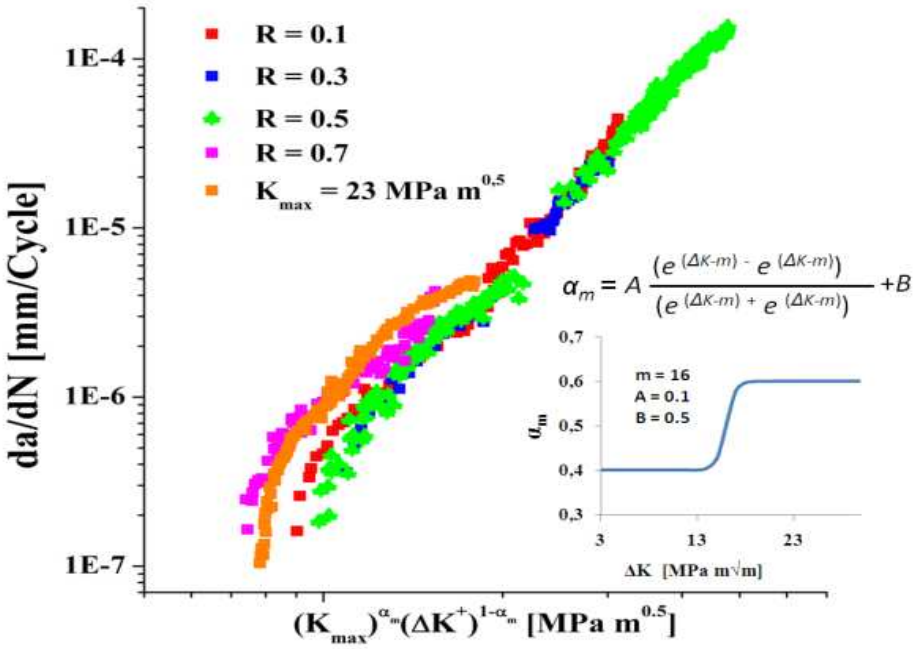

Figure 19. Fatigue crack growth rate as a function of *K*** for the annealed steel.

The following expression is proposed to account for the effects of crack closure:

$$K_m^* = (K_{max})^{\alpha_m}(\Delta K - g(y))^{1-\alpha_m} \quad \textbf{(7)}$$

Or the following, which uses a more familiar parameter:

$$K_m^* = (K_{max})^{\alpha_m}\left(\Delta K_{\frac{2}{Pi}m}\right)^{1-\alpha_m} \quad \textbf{(8)}$$

The parameter $\Delta K_{\frac{2}{Pi}m}$ is a modified expression of the parameter proposed by K. Donald *et al*. This parameter was modified to include the previous analysis and the results of **Figure 20**, which show that when the crack closure is small (P_o/P_{max} tends to R), the ratio between real closure (R_2) an ideal closure (R_1) is small. The ideal crack closure is assumed as the case where the gap in the crack is completely filled by a hard material when the load is below P_{op}. According to **Figure 20**b, the crack surface contact becomes harder contact with the increase in the relationship P_o/P_{max}. The parameter $\Delta K_{\frac{2}{Pi}m}$ is calculated using the following expression:

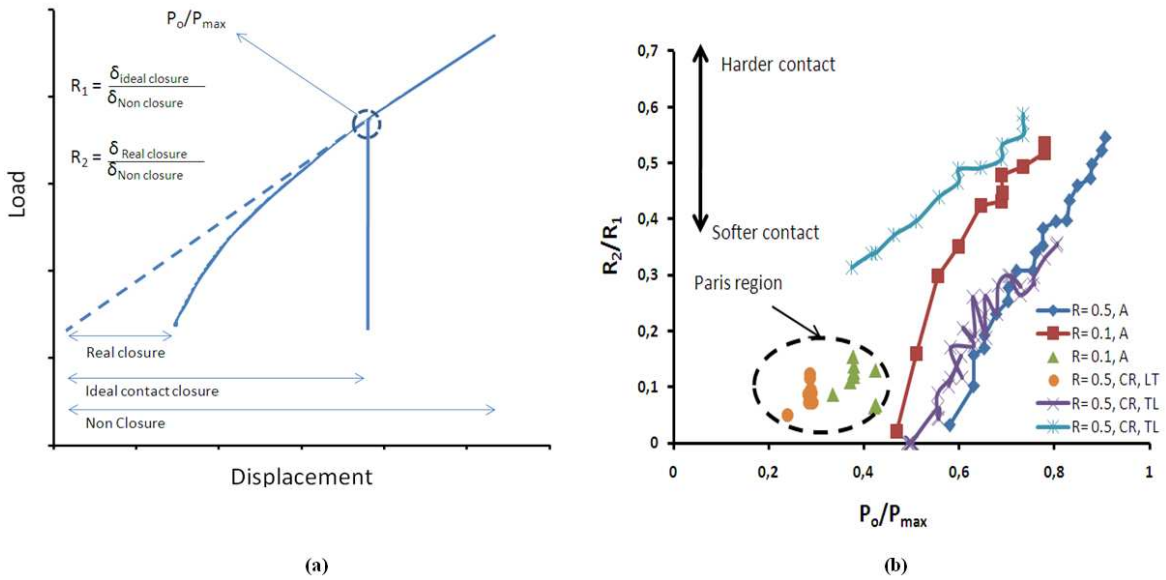

Figure 20. (a) Illustration of the load against crack opening displacement curve showing the effect of crack closure (b) Relationship between P_o/P_{max} and the change of the slope on the load-displacement curve.

$$\Delta K_{2/PIm} = \Delta K_{app} - \frac{g_m}{\pi}\left(K_{op} - K_{min}\right) \tag{9}$$

where g_m is equal to:

$$g_m\left(\frac{P_o}{P_{max}}, R\right) = Ln(d) \tag{10}$$

and *d* is a normalized expression of the relationship P_o/P_{max} and is equal to:

$$d = \left(\frac{1-R}{1-\frac{P_o}{P_{max}}}\right) \tag{11}$$

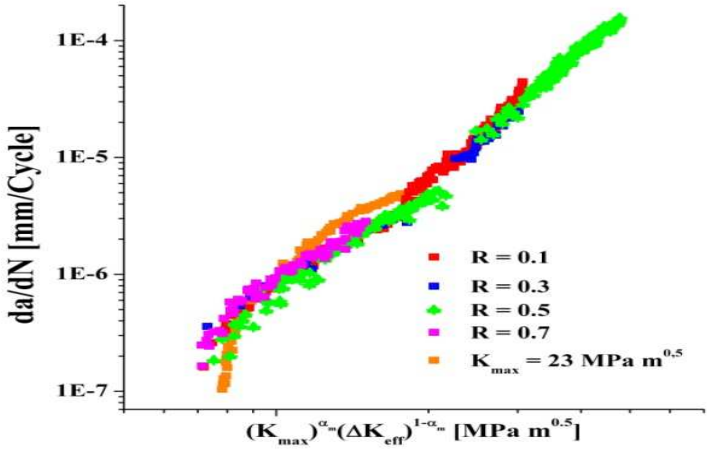

Figure 21. Fatigue crack growth rate as a function of K_m* for the annealed steel.

Figure 21 shows the correlation of the load ratio effects using equation (8). **Figure 21** indicates that the load ratio effects can be satisfactorily correlated using a parameter that includes the crack closure and the K_{max} effects, as proposed in equation (8). This same equation could be used to correlate the load ratio effects in the cold rolled steel, **Figure 22**. The curves plotted in **Figure 22** were obtained using the same α_m used for the annealed steel. This correlation could be improved for the cold rolled steel using the suitable value of α_m. However, the correlation is quite acceptable. It is not surprising that the same parameter can be used to correlate the load ratio effects in the steels in annealed and cold rolled condition, because the mechanisms that control the FCGR for both steels are the same.

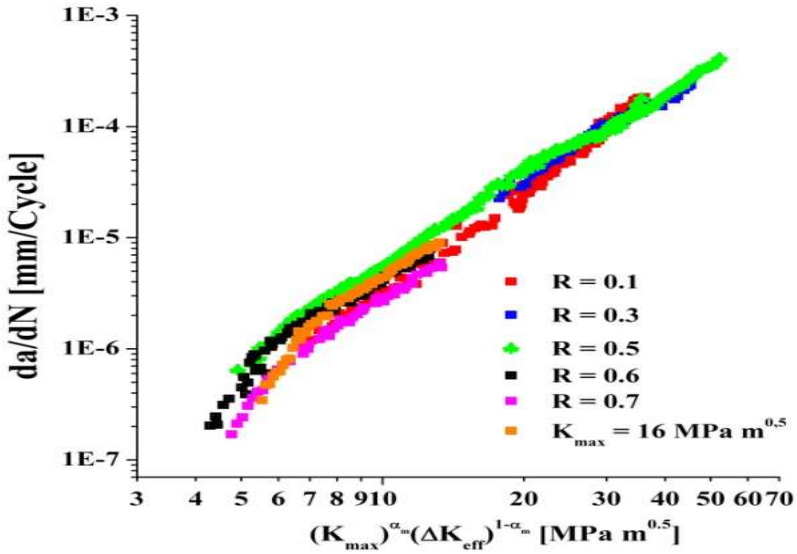

Figure 22. Fatigue crack growth rate as a function of K_m* for the cold rolled steel.

Accelerated FCGR in the cold rolled steel compared to the annealed steel is associated with the increase in the residual stress generated by the martensitic transformation [15-16], microcracks and nucleation of incipient microvoids [15-16] and the crack closure. To account for the decrease in the FCGR induced by the residual stress caused by the martensitic transformation in the Paris region, an expression was derived in the previous paper [15-16]; which is shown in equation (12), where *f(x)* is a parameter which takes into account the influence of variables that have an effect on K_{max}.

$$K_m^* = (K_{max} - f(x))^{\alpha_n}\left(\Delta K^+\right)^{1-\alpha_n} \quad \textbf{(12)}$$

Unlike the situation observed in the Paris region, where the residual stress has a substantial influence on the explanation of the lower FCGR of the annealed steel compared to the cold rolled steel, in the near threshold region the main difference between the zones of martensitic transformation in both steels is that in the cold rolled steel can be found austenite transformed to martensite prior to the tests. Therefore, the importance of the mechanism of residual stress caused by the martensitic transformation in this region is lower, when compared to the one expected in the Paris region. On the other

hand, in contrast to what happens in the Paris region, the crack path roughness is very different between the annealed steel and cold rolled steel in the near threshold region. However, and unlike the effects of residual stress which only affect the expression *f(x)* of equation (12), if the decrease caused by the crack deflection is estimated based on the analysis of Suresh [41], the crack path roughness would affect both the expression *f(x)* of equation (12) and *g(y)* of equation (7). The combination of equation (7) and (12) would result in an expression similar to:

$$\boldsymbol{K_m^* = (K_{max} - f(x))^{\alpha_m}(\Delta K - g(y))^{1-\alpha_m}} \quad \textbf{(13)}$$

The parameter proposed in equation (13), which is just an empirical parameter, can be used to explain the difference in the FCGR, as a consequence of the microstructural variables and the load ratio. In this occasion, this parameter will not be used because the effects of roughness could not be quantified, and because of the techniques used to measure the variation of the zones transformed to martensite are not suitable for a ΔK lesser than 16 Mpa√m (region where the austenite adjacent to the crack path does not transform completely to martensite). Therefore, the values of terms *f(x)* and *g (y)* cannot be adequately quantified. Future works will be aimed at finding new methods to estimate the real maximum stress intensity factor and the range of stress intensity factor in front of the crack tip. In this context, digital image correlation to estimate the stress intensity factor directly, and the two parameter model proposed by [42] seems to be promising..

6. Conclusions

The results of evaluations of the FCGR against different parameters (ΔK, ΔK_{eff}, $\Delta K_{2/Pi}$, K^*) for an MASS suggest that the influence of K_{max} (or commonly known as load ratio effects) can be explained using a combination of parameters that take into account the contribution of K_{max}, ΔK and the crack closure. To explain the difference in the FCGR, as a consequence of the microstructural variables, different mechanisms were investigated. In the Paris region, the residual stress generated by the martensitic transformation and the appearance of quasi-static fracture mode such as micro-crack formation and incipient micro-voids, seem to be the most appropriate mechanisms. In the near threshold region, the crack roughness and its implications as the crack closure induced by roughness have great influence on the difference of the FCGR of steels with different microstructural conditions. To advance in the ideas proposed, the correct quantification of all variables (roughness, internals stresses, and anticipated contact of the crack faces, among others) becomes necessary; as well as more detailed studies to understand which variable affects K_{max}, or ΔK or both, as the main driving force for fatigue crack advance.

Acknowledgements

Authors wish to express their gratitude to the funding provided by CONICET (Consejo Nacional de Investigaciones Científicas y Técnicas), and by Agencia Nacional de Promoción Científica y Tecnológica, Argentina (PICT2010 Nro.0379).

References

1 PERDAHCIOĞLU, E. S.; GEIJSELAERS, H. J. M.; HUÉTINK, J. Constitutive modeling of metastable austenitic stainless steel. *International Journal of Material Forming*, 2009, vol. 2, no 1, p. 419-422. (Doi: 10.1007/s12289-008-0037-9)

2 TOMITA, Yoshihiro; IWAMOTO, Takeshi. Constitutive modeling of TRIP steel and its application to the improvement of mechanical properties. *International Journal of Mechanical Sciences*, 1995, vol. 37, no 12, p. 1295-1305. (Doi: 10.1016/0020-7403(95)00039-Z)

3 STRINGFELLOW, R. G.; PARKS, D. M.; OLSON, G. B. A constitutive model for transformation plasticity accompanying strain-induced martensitic transformations in metastable austenitic steels. *Acta Metallurgica et Materialia*, 1992, vol. 40, no 7, p. 1703-1716. (Doi: 10.1016/0956-7151(92)90114-T)

4 BEESE, Allison M.; MOHR, Dirk. Anisotropic plasticity model coupled with Lode angle dependent strain-induced transformation kinetics law. *Journal of the Mechanics and Physics of Solids*, 2012, vol. 60, no 11, p. 1922-1940. (Doi: 10.1016/j.jmps.2012.06.009)

5 BEESE, Allison M.; MOHR, Dirk. Effect of stress triaxiality and Lode angle on the kinetics of strain-induced austenite-to-martensite transformation. *Acta Materialia*, 2011, vol. 59, no 7, p. 2589-2600. (Doi: 10.1016/j.actamat.2010.12.040)

6 TALONEN, J.; HÄNNINEN, H. Formation of shear bands and strain-induced martensite during plastic deformation of metastable austenitic stainless steels. *Acta materialia*, 2007, vol. 55, no 18, p. 6108-6118. (Doi: 10.1016/j.actamat.2007.07.015)

7 LANGE, TW CROOKERAND EA. How Yield Strength and Fracture Toughness Considerations Can Influence Fatigue Design Procedures for Structural Steels. 1970.

8 ROBERTSON, L. T.; HILDITCH, T. B.; HODGSON, P. D. The effect of prestrain and bake hardening on the low-cycle fatigue properties of TRIP steel. *International journal of fatigue*, 2008, vol. 30, no 4, p. 587-594. (Doi: 10.1016/j.ijfatigue.2007.06.002)

9 ZERBST, Uwe, et al. Fracture and damage mechanics modelling of thin-walled structures–An overview. *Engineering Fracture Mechanics*, 2009, vol. 76, no 1, p. 5-43. (Doi: 10.1016/j.engfracmech.2007.10.005)

10 PINEAU, A. G.; PELLOUX, R. M. Influence of strain-induced martensitic transformations on fatigue crack growth rates in stainless steels. *Metallurgical Transactions*, 1974, vol. 5, no 5, p. 1103-1112. (Doi: 10.1007/BF02644322)

11 MEI, Z.; MORRIS, J. W. Influence of deformation-induced martensite on fatigue crack propagation in 304-type steels. *Metallurgical Transactions A*, 1990, vol. 21, no 12, p. 3137-3152. (Doi: 10.1007/BF02647310)

12 SCHUSTER, G.; ALTSTETTER, C. Fatigue of annealed and cold worked stable and unstable stainless steels. *Metallurgical Transactions A*, 1983, vol. 14, no 10, p. 2077-2084. (Doi: 10.1007/BF02662374)

13 BISWAS, Somjeet, et al. Load history effect on FCGR behaviour of 304LN stainless steel. *International journal of fatigue*, 2007, vol. 29, no 4, p. 786-791.(DOI: 10.1016/j.ijfatigue.2006.06.003)

14 Mills, W. J., & James, L. A. Near Thershold fatigue crack Growth behavior for 316 Stainless Steel. *Journal of Testing and Evaluation* , 1987, p. 325-332.

15 MARTELO, D. F.; Mateo A. M.; Chapetti, M. D. unpublished results.

16 MARTELO, David F.; Fatiga y Fractura de Aceros Austeníticos Metaestables. 2013. Doctoral dissertation. Universidad Nacional de Mar Del Plata.

17 Suresh, S.; *Fatigue of Materials.* s.l. : Cambridge University Press, 1998. (Doi: 10.1002/adma.19930050420)

18 HEDSTRÖM, Peter. Deformation induced martensitic transformation of metastable stainless steel AISI 301. 2005.Doctoral dissertation. Luleå University of Technology.

19 BEESE, Allison M. Experimental investigation and constitutive modeling of the large deformation behavior of anisotropic steel sheets undergoing strain-induced phase transformation. 2011. Doctoral dissertation. Massachusetts Institute of Technology.

20 Talonen, J.; Effect of strain-induced α'- martensite Trasnformation on Mechanical Properties of Metastable Austenitic Stainless Steels. 2007. Doctoral dissertation. Helsinki University of Technology

21 TADA, Hiroshi; PARIS, P. C.; IRWIN, G. R. The stress analysis of cracks handbook ASME. *New*

York, 2000, p. 55-56.

22 E647-08E01, standard Test Method for Measurement of fatigue Crcak Growth Rates. *Annual Book of ASTM Standards ASTM*. Philadelphia, PA : s.n., 2010

23 ELBER, W.; The significance of fatigue crack closure. *ASTM STP 486. Damage tolerance in aircraft structures.* 1971, p. 230-242.

24 PARIS, Paul C.; TADA, Hiroshi; DONALD, J. Keith. Service load fatigue damage—a historical perspective. *International Journal of fatigue*, 1999, vol. 21, p. S35-S46. (Doi: 10.1016/S0142-1123(99)00054-7)

25 KUJAWSKI, Daniel. A new (ΔK, K_{max}) driving force parameter for crack growth in aluminum alloys. *International Journal of Fatigue*, 2001, vol. 23, no 8, p. 733-740. (Doi: 10.1016/S0142-1123(01)00023-8)

26 SHIN, C. S.; SMITH, R. A. Fatigue crack growth from sharp notches.*International journal of fatigue*, 1985, vol. 7, no 2, p. 87-93. (Doi: 10.1016/0142-1123(85)90038-6)

27 MACHA, D. E.; CORBLY, D. M.; JONES, J. W. On the variation of fatigue-crack-opening load with measurement location. *Experimental Mechanics*, 1979, vol. 19, no 6, p. 207-213. (Doi: 10.1007/BF02324983)

28 ZHANG, Jia-zhen; HE, X. D.; DU, S. Y. Analyses of the fatigue crack propagation process and stress ratio effects using the two parameter method.*International journal of fatigue*, 2005, vol. 27, no 10, p. 1314-1318. (Doi: 10.1016/j.ijfatigue.2005.06.010)

29 BRAY, G. H.; DONALD, K. J.; Separating the influence of Kmax from closure-related stress ratio effects using the adjusted compliance ratio tecnique. *ASTM STP 1343, Advances in Fatigue Crack Closure Measurement and Analysis.* 1999, p. 57-78.

30 KUJAWSKI, D.; ELLYIN, F. A fatigue crack growth model with load ratio effects. *Engineering fracture mechanics*, 1987, vol. 28, no 4, p. 367-378. (Doi: 10.1016/0013-7944(87)90182-2)

31 VASUDEVAN, A. K.; SADANANDA, K.; LOUAT, N. Reconsideration of fatigue crack closure. *Scripta metallurgica et materialia*, 1992, vol. 27, no 11, p. 1673-1678. (Doi: 10.1016/0956-716X(92)90164-A)

32 VASUDEVAN, A. K.; SADANANDA, K.; LOUAT, N. Two critical stress intensities for threshold fatigue crack propagation. *Scripta metallurgica et materialia*, 1993, vol. 28, no 1, p. 65-70. (Doi: 10.1016/0956-716X(93)90538-4)

33 VASUDEVAN, A. K.; SADANANDA, K. Classification of fatigue crack growth

behavior. *Metallurgical and Materials Transactions A*, 1995, vol. 26, no 5, p. 1221-1234. (Doi: 10.1007/BF02670617)

34 MCEVILY, A. J.; RITCHIE, R. O. Crack closure and the fatigue-crack propagation threshold as a function of load ratio. *Fatigue and Fracture of Engineering Materials and Structures*, 1998, vol. 21, p. 847-856. (Doi: 10.1046/j.1460-2695.1998.00069.x)

35 VASUDEVEN, A. K.; SADANANDA, K.; LOUAT, N. A review of crack closure, fatigue crack threshold and related phenomena. *Materials Science and Engineering: A*, 1994, vol. 188, no 1, p. 1-22. (Doi: 10.1016/0921-5093(94)90351-4)

36 PIPPAN, Reinhard. Threshold and effective threshold of fatigue crack propagation in ARMCO iron I: the influence of grain size and cold working.*Materials Science and Engineering: A*, 1991, vol. 138, no 1, p. 1-13.

37 NAKAJIMA, K.; YOKOE, M.; MIYATA, T.; The effect of Microstructure and prestrain on fatigue crack propagation of dual phase steels. p. 1541- 1548.

38 GAO, Ming; CHEN, Shuchun; WEI, Robert P. Crack paths, microstructure, and fatigue crack growth in annealed and cold-rolled AISI 304 stainless steels. *Metallurgical Transactions A*, 1992, vol. 23, no 1, p. 355-371. (Doi: 10.1007/BF02660877)

39 SADANANDA, K.; VASUDEVAN, A. K. Crack tip driving forces and crack growth representation under fatigue. *International Journal of Fatigue*, 2004, vol. 26, no 1, p. 39-47. (Doi: 10.1016/S0142-1123(03)00105-1)

40 KALNAUS, S., et al. An experimental investigation of fatigue crack growth of stainless steel 304L. *International Journal of Fatigue*, 2009, vol. 31, no 5, p. 840-849. (Doi: 10.1016/j.ijfatigue.2008.11.004)

41 SURESH, S. Crack deflection: implications for the growth of long and short fatigue cracks. *Metallurgical Transactions A*, 1983, vol. 14, no 11, p. 2375-2385. (Doi: 10.1007/BF02663313)

42 NOROOZI, A. H.; GLINKA, G.; LAMBERT, S. A two parameter driving force for fatigue crack growth analysis. *International Journal of Fatigue*, 2005, vol. 27, no 10, p. 1277-1296. (Doi: 10.1016/j.ijfatigue.2005.07.002)